Polarized absorption spectra of $Eu(BrO_3)_3 \cdot 9H_2O$

1996 J. Phys.: Condens. Matter 8 1267

(http://iopscience.iop.org/0953-8984/8/9/017)

J. Phys.: Condens. Matter **8** (1996) 1267–1279. Printed in the UK

Polarized absorption spectra of $Eu(BrO_3)_3 \cdot 9H_2O$

K Binnemans and C Görller-Walrand

Katholieke Universiteit Leuven, Department of Chemistry, Coordination Chemistry Division, Celestijnenlaan 200F, B-3001 Heverlee, Belgium

Received 12 September 1995, in final form 27 November 1995

Abstract. The polarized absorption spectra of europium bromate enneahydrate $Eu(BrO_3)_3 \cdot 9H_2O$ have been recorded at ambient temperature and at 77 K between 16 500 and 36 000 cm^{-1}. The site symmetry is approximated by a D_{3h} symmetry. 63 crystal field levels have been assigned. The energy level scheme is parametrized in terms of 20 free ion parameters and four crystal field parameters. The crystal field parameters are $B_0^2 = 205$ cm^{-1}, $B_0^4 = -279$ cm^{-1}, $B_0^6 = -557$ cm^{-1} and $B_6^6 = -872$ cm^{-1}. Because of the weak crystal field felt by the Eu^{3+} ion, J-mixing is not very important in the bromate matrix. A consequence is that most of the observed induced electric dipole transitions starting from the $^7F_0$ level obey the $|\Delta J| = 2$, 4, 6 selection rules of the Judd–Ofelt theory. Comparison with other Eu^{3+} systems enables us to conclude that a tricapped trigonal prism as a coordination polyhedron (C.N. = 9) results in weak crystal fields, regardless of the chemical nature of the ligands.

1. Introduction

Since the fine structure of the absorption and luminescence spectra of a trivalent lanthanide ion is very sensitive to the symmetry of the immediate environment around the ion, it has been proposed to use the lanthanide ions as spectroscopic probes for a detailed structural study of both crystalline and non-crystalline compounds [1]. Especially the Eu^{3+} ion is very suitable as a probe, because of its non-degenerate ground state, the absence of overlap of the $^{2S+1}L_J$ multiplets in the 0–25 000 cm^{-1} spectral region and the small J-values of the multiplets. This facilitates the interpretation of Eu^{3+} spectra compared to the spectra of other lanthanide ions. Even at room temperature the 4f–4f transitions of Eu^{3+} have small line widths so the different crystal field transitions within one multiplet are in most cases well separated. The possibility of probing the rare earth site at ambient temperatures is important for the study of crystalline host matrices which undergo a phase transition at cryogenic conditions. The isomorphous series of the lanthanide bromate enneahydrates, $Ln(BrO_3)_3 \cdot 9H_2O$, is an example of such a matrix. Helmholtz [2] has determined the crystal structure of $Nd(BrO_3)_3 \cdot 9H_2O$ and found that the coordination polyhedron around the neodymium ion is a slightly distorted tricapped trigonal prism with C_{3v} symmetry, but not far from the ideal D_{3h} symmetry. Hellwege and Kahle [3] concluded from the temperature dependence of the $^5D_1 \leftarrow {}^7F_0$ and $^5D_2 \leftarrow {}^7F_0$ transitions in the absorption spectrum of $Eu(BrO_3)_3 \cdot 9H_2O$ that the crystal is not hexagonal but pseudohexagonal. The deviation from the hexagonal symmetry is too small to be detected by x-ray diffraction. According to these authors, the crystal is composed of six sectors, which are monoclinic above 67 K and triclinic beneath 67 K. At decreasing temperature, a progressive splitting of the levels is noticed, indicating an increasing distortion. The presence of more than $2J + 1$ lines within

0953-8984/96/091267+13$19.50

one $^{2S+1}L_J$ multiplet at low temperatures proves the existence of several non-equivalent sites in the crystal. Satten [4] recorded the absorption spectrum of $Nd(BrO_3)_3 \cdot 9H_2O$ at room and liquid-nitrogen temperature. He explained the spectrum within a C_{3v} symmetry. Transitions in the spectrum showed a mixed electric and magnetic dipole character. Sikka [5] has solved the crystal structure of $Sm(BrO_3)_3 \cdot 9H_2O$ by neutron diffraction and found a D_{3h} symmetry for the Sm^{3+} site. Structure determination of $Pr(BrO_3)_3 \cdot 9H_2O$ and $Yb(BrO_3)_3 \cdot 9H_2O$ by Albertsson and Elding [6] also revealed a regular tricapped trigonal prism with symmetry D_{3h} for the coordination polyhedron. Polarized Raman spectra and infrared absorption spectra of $La(BrO_3)_3 \cdot 9H_2O$ and $Nd(BrO_3)_3 \cdot 9H_2O$ have been recorded by Kato *et al* [7]. The properties of the $Ln(BrO_3)_3 \cdot 9H_2O$ compounds published before 1978 have been reviewed in *Gmelin Handbuch der Anorganischen Chemie* [8]. Hasunuma *et al* [9] have measured the polarized fluorescence of $Eu(BrO_3)_3 \cdot 9H_2O$ between 12 000 and 20 000 cm^{-1} at 95 K with Ar^+ laser excitation. For the spectral assignments and theoretical calculations a D_3 symmetry instead of D_{3h} was adopted, since the authors argue that labelling is more convenient in the former symmetry. Crystal field levels are given for the ^7F_J (J from 0 to 6) and the ^5D_J ($J = 0$ and 1) multiplets. The transition intensities of the fluorescence spectra have also been parametrized. Moret *et al* [10] reported a structural and luminescence study of $Eu(BrO_3)_3 \cdot 9H_2O$ and $Tb(BrO_3)_3 \cdot 9H_2O$. The site symmetry is lowered from D_{3h} to C_{3v} by a decrease of the temperature from 295 K to 200 K. The terbium compound deviates more from the D_{3h} symmetry than the europium compound. The luminescence spectra at 77 K could be explained within a C_{3v} symmetry. The spectra at lower temperature revealed a phase transition and in the luminescence spectra at 4.2 K four non-equivalent sites could be distinguished.

In this paper, we present the polarized orthoaxial absorption spectra of $Eu(BrO_3)_3 \cdot 9H_2O$ between 16 500 and 36 000 cm^{-1} at ambient temperatures and 77 K. The 4f–4f transitions are assigned assuming a D_{3h} symmetry. A set of 20 free ion parameters and four crystal field parameters is optimized. This work has been performed as a continuation of our work on Eu^{3+} systems, e.g. $Eu_2Zn_3(NO_3)_{12} \cdot 24H_2O$ [11], $LiYF_4 : Eu^{3+}$ [12], EuODA [13], $YAl_3(BO_3)_4 : Eu^{3+}$ [14] and $GdAl_3(BO_3)_4 : Eu^{3+}$ [15].

2. Experimental details

Single crystals of $Eu(BrO_3)_3 \cdot 9H_2O$ were prepared by mixing an aqueous solution of $Ba(BrO_3)_2$ and an aqueous solution of $Eu_2(SO_4)_3 \cdot 8H_2O$ in a 3:1 molar ratio. The precipitation of $BaSO_4$ was filtered and the clear solution was allowed to evaporate slowly. After several recrystallizations, small colourless prismatic crystals were formed. These crystals were suitable for recording orthoaxial (σ, π) spectra. The crystal faces were polished by etching on a wet filter paper. The optical path length of the sample was 1.8 mm. The absorption spectra were recorded at ambient temperatures and at 77 K on an AVIV 17DS spectrophotometer. Light polarization was achieved by a Glan–Thompson polarizer. For the low-temperature measurements, the sample was cooled with liquid nitrogen in a continuous flow cryostat (Oxford Instruments).

3. Selection rules

Because the work of Moret *et al* [10] reveals that the Eu^{3+} in $Eu(BrO_3)_3 \cdot 9H_2O$ at 295 K is situated in a site with D_{3h} symmetry, the selection rules for induced electric dipole (ED) and magnetic dipole (MD) transitions in a D_{3h} symmetry were deduced (table 1). The

crystal field levels in a D_{3h} symmetry have the symmetry labels Γ_1, Γ_2, Γ_3, Γ_4, Γ_5 and Γ_6 according to the notations of Koster *et al* [16]. σ and π are defined in the usual manner: σ spectrum, $\boldsymbol{c} \perp \boldsymbol{z}$, $\boldsymbol{E} \perp \boldsymbol{c}$ and $\boldsymbol{H} \| \boldsymbol{c}$; π spectrum, $\boldsymbol{c} \perp \boldsymbol{z}$, $\boldsymbol{E} \| \boldsymbol{c}$ and $\boldsymbol{H} \perp \boldsymbol{c}$. $\boldsymbol{z}$ is the propagation direction of the light and $\boldsymbol{c}$ is the main crystal axis. $\boldsymbol{E}$ and $\boldsymbol{H}$ are the electric and magnetic field vectors of the incident light respectively. All transitions in the absorption spectrum at ambient temperatures start from the $^7F_0$ or the $^7F_1$ level. The $^7F_0$ ground state has symmetry label Γ_1 and the $^7F_1$ level is split into a Γ_2 and a Γ_5 crystal field level. Since most transitions in the Eu^{3+} spectrum are ED transitions, it is clear from the selection rules for ED transitions in a D_{3h} symmetry that only crystal field levels with symmetry labels Γ_4 and Γ_6 can be observed for transitions starting from the ground state. At 77 K all transitions start from the $^7F_0$ ground state and it is then only possible to detect labels with a Γ_4 or Γ_6 symmetry.

Table 1. Selection rules for induced ED and MD transitions in a D_{3h} symmetry.

ED	Γ_1	Γ_2	Γ_3	Γ_4	Γ_5	Γ_6	MD	Γ_1	Γ_2	Γ_3	Γ_4	Γ_5	Γ_6
Γ_1	—	—	—	π	—	$\sigma+\alpha$	Γ_1	—	σ	—	—	$\pi+\alpha$	—
Γ_2	—	—	π	—	—	$\sigma+\alpha$	Γ_2	σ	—	—	—	$\pi+\alpha$	—
Γ_3	—	π	—	—	$\sigma+\alpha$	—	Γ_3	—	—	—	σ	—	$\pi+\alpha$
Γ_4	π	—	—	—	$\sigma+\alpha$	—	Γ_4	—	—	σ	—	—	$\pi+\alpha$
Γ_5	—	—	$\sigma+\alpha$	$\sigma+\alpha$	$\sigma+\alpha$	π	Γ_5	$\pi+\alpha$	$\pi+\alpha$	—	—	σ	$\pi+\alpha$
Γ_6	$\sigma+\alpha$	$\sigma+\alpha$	—	—	π	$\sigma+\alpha$	Γ_6	—	—	$\pi+\alpha$	$\pi+\alpha$	$\pi+\alpha$	σ

The number and symmetry of crystal field levels in which each $^{2S+1}L_J$ is split by the crystal field perturbating the 4f configuration can be found in the full-rotation group compatibility table for a D_{3h} symmetry [16]. In order to fulfil the selection rules, the $^5D_1 \leftarrow {}^7F_0$ transition has to show one peak in σ and one peak in π, the $^5D_2 \leftarrow {}^7F_0$ one peak in σ, the $^5D_4 \leftarrow {}^7F_0$ transition two peaks in σ and one peak in π and the $^5L_6 \leftarrow {}^7F_0$ transition also has two peaks in σ and one peak in π.

4. Analysis of the polarized spectra

The polarized absorption spectra of $Eu(BrO_3)_3 \cdot 9H_2O$ at ambient temperature between 16 500 and 36 000 cm^{-1} are given in figures 1–6. Above 36 000 cm^{-1}, a strong light absorption by the bromate matrix prevented the detection of 4f–4f transitions. Observation of the transitions to $^7F_5$ and $^7F_6$ ($\sim$ 4000–5000 cm^{-1} in the near infrared) was not possible because of the overtones and combination bands of the vibrations of the bromate and water molecules. The 4f–4f transitions are ED transitions, except the $^5D_0 \leftarrow {}^7F_1$ ($\sim$ 16 850 cm^{-1}) and the $^5D_1 \leftarrow {}^7F_0$ ($\sim$ 19 000 cm^{-1}) transitions, which are MD transitions. The most intense transition is the $^5L_6 \leftarrow {}^7F_0$ transition at $\sim$ 25 200 cm^{-1}, followed by the $^5H_{6,5} \leftarrow {}^7F_0$ transition at $\sim$ 31 500 cm^{-1}. The hypersensitive $^5D_2 \leftarrow {}^7F_0$ transition ($\sim$ 21 500 cm^{-1}) is weak, compared with the $^5D_1 \leftarrow {}^7F_0$ transition. A total of 63 crystal field transitions have been detected in the spectra. The crystal field transitions in the polarized absorption spectra of $Eu(BrO_3)_3 \cdot 9H_2O$ are summarized in table 2. The transitions are well polarized, although some polarization leaks can be observed, e.g. the peak at 21 485 cm^{-1} ($^5D_2 \leftarrow {}^7F_0$). The assignments are made for the transitions in the spectra at ambient temperature. The spectra at 77 K were used to discriminate between transitions starting from the $^7F_0$ level and those starting from the first excited level $^7F_1$. This is important for the transitions in the energy region above 25 000 cm^{-1}. Due to the high density of states, transitions starting from the

Table 2. Transitions in the polarized absorption spectrum of $Eu(BrO_3)_3 \cdot 9H_2O$ at ambient temperatures.

Energy (cm^{-1})	Polarization	Transition	Assignment
16 842	σ	$^5D_0 \leftarrow {}^7F_1$	$\Gamma_1 \leftarrow \Gamma_2$
16 896	π	$^5D_0 \leftarrow {}^7F_1$	$\Gamma_1 \leftarrow \Gamma_5$
19 010	π	$^5D_1 \leftarrow {}^7F_0$	$\Gamma_5 \leftarrow \Gamma_1$
19 019	σ	$^5D_1 \leftarrow {}^7F_0$	$\Gamma_2 \leftarrow \Gamma_1$
21 485	σ^*	$^5D_2 \leftarrow {}^7F_0$	$\Gamma_6 \leftarrow \Gamma_1$
23 938	σ	$^5D_3 \leftarrow {}^7F_1$	$\Gamma_6 \leftarrow \Gamma_2$
23 989	π	$^5D_3 \leftarrow {}^7F_1$	$\Gamma_6 \leftarrow \Gamma_5$
24 003	σ	$^5D_3 \leftarrow {}^7F_1$	$\Gamma_5 \leftarrow \Gamma_5$
24 723	σ	$^5L_6 \leftarrow {}^7F_1$	$\Gamma_5^a \leftarrow \Gamma_5$
24 740	π	$^5L_6 \leftarrow {}^7F_1$	$\Gamma_3 \leftarrow \Gamma_2$
24 818	σ	$^5L_6 \leftarrow {}^7F_1$	$\Gamma_5 \leftarrow \Gamma_5$
24 911	π	$^5L_6 \leftarrow {}^7F_1$	$\Gamma_6 \leftarrow \Gamma_5$
24 945	σ	$^5L_6 \leftarrow {}^7F_1$	$\Gamma_4 \leftarrow \Gamma_5$
25 129	σ	$^5L_6 \leftarrow {}^7F_0$	$\Gamma_6^a \leftarrow \Gamma_1$
25 263	σ	$^5L_6 \leftarrow {}^7F_0$	$\Gamma_6^b \leftarrow \Gamma_1$
25 299	π	$^5L_6 \leftarrow {}^7F_0$	$\Gamma_4 \leftarrow \Gamma_1$
25 857	σ	$(^5L_7, {}^5G_2) \leftarrow {}^7F_1$	$\Gamma_4 \leftarrow \Gamma_5$
25 873	π	$(^5L_7, {}^5G_2) \leftarrow {}^7F_1$	$\Gamma_6 \leftarrow \Gamma_5$
25 944	π	$(^5L_7, {}^5G_2) \leftarrow {}^7F_1$	$\Gamma_6 \leftarrow \Gamma_5$
26 049	σ	$(^5L_7, {}^5G_2) \leftarrow {}^7F_1$	$\Gamma_5 \leftarrow \Gamma_5$
26 204	π	$(^5L_7, {}^5G_2) \leftarrow {}^7F_0$	$\Gamma_4 \leftarrow \Gamma_1$
26 249	σ	$(^5L_7, {}^5G_2) \leftarrow {}^7F_0$	$\Gamma_6 \leftarrow \Gamma_1$
26 269	π	$(^5L_7, {}^5G_2) \leftarrow {}^7F_0$	$\Gamma_4 \leftarrow \Gamma_1$
26 517	π	$^5G_3 \leftarrow {}^7F_0$	$\Gamma_4 \leftarrow \Gamma_1$
26 600	π	$^5G_{4,5,6} \leftarrow {}^7F_0$	$\Gamma_4 \leftarrow \Gamma_1$
26 640	σ	$^5G_{4,5,6} \leftarrow {}^7F_0$	$\Gamma_6 \leftarrow \Gamma_1$
26 667	π	$^5G_{4,5,6} \leftarrow {}^7F_0$	$\Gamma_4 \leftarrow \Gamma_1$
26 728	σ	$^5G_{4,5,6} \leftarrow {}^7F_0$	$\Gamma_6 \leftarrow \Gamma_1$
27 150	π	$^5D_4 \leftarrow {}^7F_1$	$\Gamma_3 \leftarrow \Gamma_2$
27 198	σ	$^5D_4 \leftarrow {}^7F_1$	$\Gamma_6 \leftarrow \Gamma_2$
27 239	σ	$^5D_4 \leftarrow {}^7F_1$	$\Gamma_4 \leftarrow \Gamma_5$
27 272	π	$^5D_4 \leftarrow {}^7F_1$	$\Gamma_6 \leftarrow \Gamma_5$
27 591	σ	$^5D_4 \leftarrow {}^7F_0$	$\Gamma_6^a \leftarrow \Gamma_1$
27 592	π	$^5D_4 \leftarrow {}^7F_0$	$\Gamma_4 \leftarrow \Gamma_1$
27 630	σ	$^5D_4 \leftarrow {}^7F_0$	$\Gamma_6^b \leftarrow \Gamma_1$
30 570	σ	$^5H_3 \leftarrow {}^7F_1$	$\Gamma_3 \leftarrow \Gamma_5$
30 624	σ	$^5H_7 \leftarrow {}^7F_1$	$\Gamma_5 \leftarrow \Gamma_5$
31 000	π	$^5H_7 \leftarrow {}^7F_0$	$\Gamma_4 \leftarrow \Gamma_1$
31 058	σ	$^5H_7 \leftarrow {}^7F_0$	$\Gamma_6 \leftarrow \Gamma_1$
31 095	π	$^5H_7 \leftarrow {}^7F_0$	$\Gamma_4 \leftarrow \Gamma_1$
31 148	σ	$^5H_7 \leftarrow {}^7F_0$	$\Gamma_6 \leftarrow \Gamma_1$
31 176	π	$^5H_{6,5} \leftarrow {}^7F_1$	$\Gamma_6 \leftarrow \Gamma_5$
31 237	π	$^5H_{6,5} \leftarrow {}^7F_1$	$\Gamma_6 \leftarrow \Gamma_5$
31 269	σ	$^5H_{6,5} \leftarrow {}^7F_1$	$\Gamma_4 \leftarrow \Gamma_5$
31 468	π	$^5H_{6,5} \leftarrow {}^7F_0$	$\Gamma_4 \leftarrow \Gamma_1$
31 531	σ	$^5H_{6,5} \leftarrow {}^7F_0$	$\Gamma_6 \leftarrow \Gamma_1$
32 574	π	$^5F_{3,2} \leftarrow {}^7F_1$	$\Gamma_3 \leftarrow \Gamma_2$
32 693	σ	$^5F_{3,2} \leftarrow {}^7F_1$	$\Gamma_5 \leftarrow \Gamma_5$
32 724	π	$^5F_{3,2} \leftarrow {}^7F_1$	$\Gamma_6 \leftarrow \Gamma_5$
33 029	σ	$^5F_{3,2} \leftarrow {}^7F_0$	$\Gamma_6 \leftarrow \Gamma_1$
33 177	π	$^5F_4 \leftarrow {}^7F_1$	$\Gamma_6 \leftarrow \Gamma_5$
33 369	π	$^5F_1 \leftarrow {}^7F_0$	$\Gamma_5 \leftarrow \Gamma_1$

Table 2. (Continued)

Energy (cm^{-1})	Polarization	Transition	Assignment
33 454	σ	$^5F_4 \leftarrow {}^7F_0$	$\Gamma_6 \leftarrow \Gamma_1$
33 471	π	$^5F_4 \leftarrow {}^7F_0$	$\Gamma_4 \leftarrow \Gamma_1$
33 630	σ	$^5F_5 \leftarrow {}^7F_1$	$\Gamma_5 \leftarrow \Gamma_5$
33 694	π	$^5I_4 \leftarrow {}^7F_1$	$\Gamma_6 \leftarrow \Gamma_5$
33 944	σ	$^5F_5 \leftarrow {}^7F_0$	$\Gamma_6 \leftarrow \Gamma_1$
33 981	π	$^5I_4 \leftarrow {}^7F_0$	$\Gamma_4 \leftarrow \Gamma_1$
34 036	σ	$^5F_5 \leftarrow {}^7F_0$	$\Gamma_6 \leftarrow \Gamma_1$
34 111	σ	$^5I_4 \leftarrow {}^7F_0$	$\Gamma_6 \leftarrow \Gamma_1$
34 945	σ	$^5I_6 \leftarrow {}^7F_0$	$\Gamma_6 \leftarrow \Gamma_1$
34 969	π	$^5I_6 \leftarrow {}^7F_0$	$\Gamma_4 \leftarrow \Gamma_1$
35 032	σ	$^5I_6 \leftarrow {}^7F_0$	$\Gamma_6 \leftarrow \Gamma_1$

* Due to a depolarization effect, this transition is detected also as a weak peak in the π-spectrum.

$^7F_0$ and $^7F_1$ are often not well separated. No evidence for a symmetry lowering from D_{3h} to C_{3v} was observed in our spectra after cooling to 77 K (liquid nitrogen temperature). It is of course possible that a symmetry lowering occurs, but in that case the additional lines in a C_{3v} symmetry have such a low intensity that they cannot be detected by absorption spectroscopy. Assignments in spectral regions with a high density of energy levels were only possible with the aid of the calculated energy level scheme. Difficult regions are 26 000–27 200 cm^{-1} ($^5L_7$, $^5G_2$, $^5G_3$, $^5G_4$, $^5G_5$, $^5G_6$ and $^5L_8$) and 32 800–35 100 cm^{-1} ($^3P_0$, $^5F_1$, $^5F_6$, $^5I_4$, $^5I_5$, $^5I_6$).

5. The energy level scheme and crystal field parametrization

The total Hamiltonian can be written as a free ion part and a crystal field part:

$$H = H_{free\ ion} + H_{crystal\ \ field}. \tag{1}$$

The free ion Hamiltonian is characterized by a set of free electron repulsion parameters (F^2, F^4, F^6), by the spin–orbit coupling constant ζ_{4f}, the Trees configuration interaction parameters (α, β, γ), the three-body configuration interaction parameters (T^2, T^3, T^4, T^6, T^7, T^8) and parameters which describe magnetic interactions (M^0, M^2, M^4, P^2, P^4, P^6) a further parameter E_{ave} takes into account the kinetic energy of the electrons and their interactions with the nucleus. It shifts only the barycentre of the whole 4f configuration. So one can write [17]

$$\begin{aligned} H_{free\ ion} = {} & E_{ave} + \sum_k F^k f_k + \zeta_{4f} A_{SO} + \alpha L(L+1) + \beta G(G_2) + \gamma G(R_7) \\ & + \sum_i T^i t_i + \sum_k P^k p_k + \sum_l M^l m_l \\ & i = 2, 3, 4, 6, 7, 8 \qquad k = 2, 4, 6 \qquad l = 0, 2, 4. \end{aligned} \tag{2}$$

f_k and A_{SO} represent the angular part of the electrostatic and spin–orbit interaction respectively. L is the total orbital angular momentum. $G(G_2)$ and $G(R_7)$ are the Casimir operators for the groups G_2 and R_7. The t_i are the three-particle operators. p_k and m_l represent the operators for the magnetic corrections.

For a D_{3h} symmetry, the even part of the crystal field Hamiltonian is expanded as [18]

$$H_{D_3}^{even} = B_0^2 C_0^2 + B_0^4 C_0^4 + B_0^6 C_0^6 + B_6^6 [C_{-6}^6 + C_6^6]. \tag{3}$$

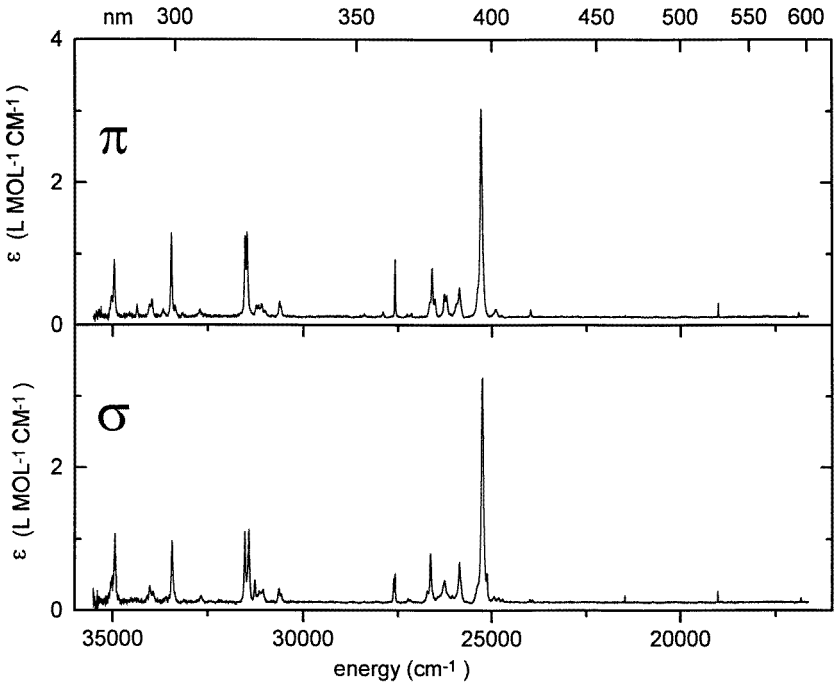

Figure 1. The (σ, π)-polarized absorption spectra of $Eu(BrO_3)_3 \cdot 9H_2O$ at ambient temperature: overview.

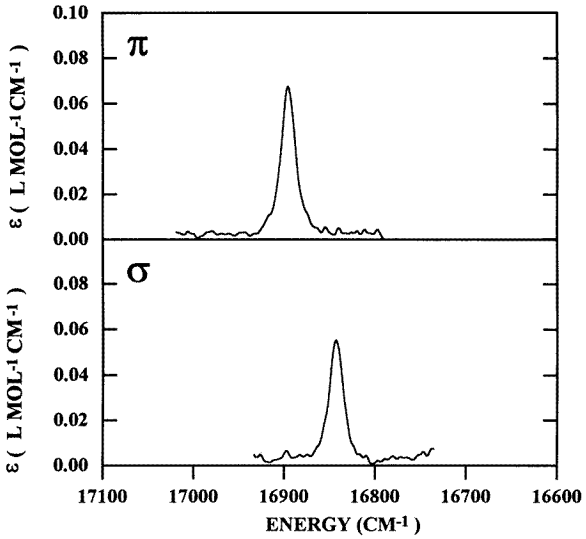

Figure 2. The $^5D_0 \leftarrow {}^7F_1$ transition in the polarized absorption spectra of $Eu(BrO_3)_3 \cdot 9H_2O$ at ambient temperature.

The C_q^k are spherical tensor operators of rank k with components q. The B_q^k are the crystal field parameters. Our choice of the coordinate axes (Y-axis parallel to the twofold axis)

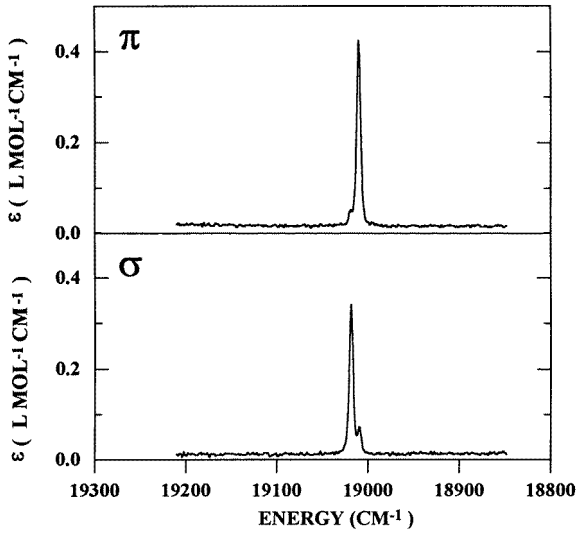

Figure 3. The $^5D_1 \leftarrow {}^7F_0$ transition in the polarized absorption spectra of $Eu(BrO_3)_3 \cdot 9H_2O$ at ambient temperature.

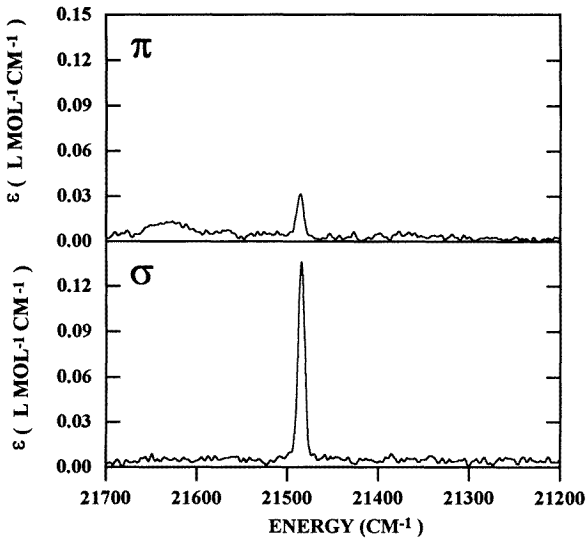

Figure 4. The $^5D_2 \leftarrow {}^7F_0$ transition in the polarized absorption spectra of $Eu(BrO_3)_3 \cdot 9H_2O$ at ambient temperature.

implicates that the B_6^6 parameter is negative, in contrast to the value reported by Hasunuma *et al* [9]. The parameter set is determined by optimizing a starting set. This is done by minimizing the squares of the differences between the experimental and calculated crystal field levels. As starting values for the free ion parameters, the mean free ion parameters for Eu^{3+} reported by Görller-Walrand and Binnemans are chosen [19]. The starting crystal field parameters are those of Hasunuma *et al* [9], omitting the B_3^4 and B_3^6 parameters, which are absent from a D_{3h} symmetry. In the fitting procedure, the crystal field levels for the ^7F_J

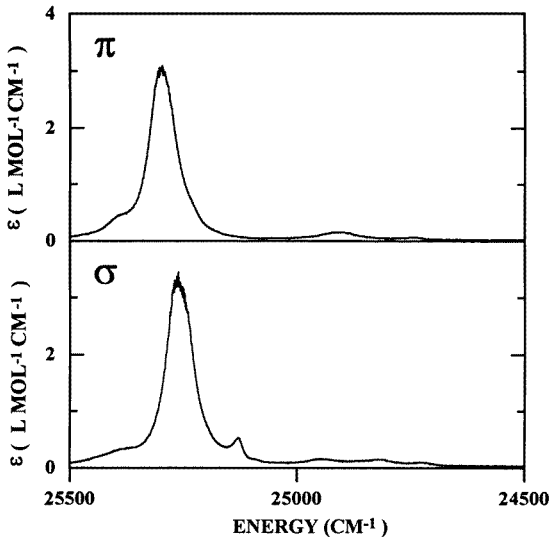

Figure 5. The $^5L_6 \leftarrow {}^7F_{0,1}$ transitions in the polarized absorption spectra of $Eu(BrO_3)_3 \cdot 9H_2O$ at ambient temperature.

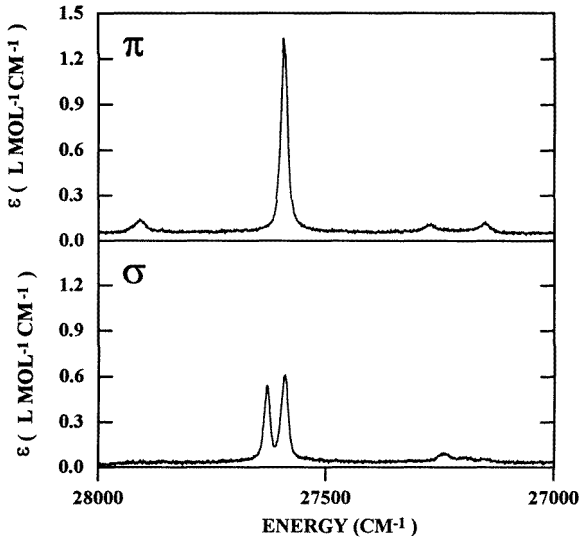

Figure 6. The $^5D_4 \leftarrow {}^7F_{0,1}$ transitions in the polarized absorption spectra of $Eu(BrO_3)_3 \cdot 9H_2O$ at ambient temperature.

multiplets reported by Hasunuma *et al* [9] were added to our set of experimental crystal field levels. It was assumed that the symmetry lowering from D_{3h} to C_{3v} when the temperature decreases will only have an influence on the selection rules (i.e. more transitions will be found in a C_{3v} symmetry than in a D_{3h} symmetry) and will not change the position of the crystal field levels significantly. The ^7F_J levels are important for the determination of the spin–orbit coupling parameter ζ_{4f}. The parameters F^2, F^4, F^6, T^3, T^4, T^6, T^7, P^2, P^4

and P^6 were constrained during the fitting procedure. The M^k and P^k parameters are in the pseudo-relativistic Hartree–Fock ratios $M^2/M^0 = 0.56$, $M^4/M^0 = 0.38$, $P^4/P^2 = 0.75$ and $P^6/P^2 = 0.50$ [20]. The r.m.s. value (σ-value) of the last fit was 10.6 cm^{-1}. A trial to fit the energy levels in a C_{3v} symmetry has not given better results. The final parameter set can be found in table 3. In table 4, the experimental and calculated crystal field levels are given.

Table 3. Free ion and crystal field parameters (in a D_{3h} symmetry) for Eu^{3+} in $Eu(BrO_3)_3 \cdot 9H_2O$. The parameters between square brackets were constrained during the fit. The values between parentheses are the r.m.s. errors on the parameters which were allowed to vary freely.

Parameter	Value (cm^{-1})	Parameter	Value (cm^{-1})
E_{ave}	63 742 (2)	ζ_{4f}	1334.0 (1.9)
F^2	[82 786]	M^0	2.612 (0.114)
F^4	[59 401]	M^2	0.56 M^0
F^6	[42 644]	M^4	0.38 M^0
α	19.996 (0.126)	P^2	[303]
β	−619 (21)	P^4	0.75 P^2
γ	1461 (37)	P^6	0.50 P^2
T^2	335 (8)	B_0^2	205 (17)
T^3	[40]	B_0^4	−279 (35)
T^4	[40]	B_0^6	−557 (49)
T^6	[−330]	B_6^6	−872 (27)
T^7	[380]		
T^8	365 (22)		

6. Discussion and conclusions

The energy level scheme of Eu^{3+} in the bromate enneahydrate matrix $Eu(BrO_3)_3 \cdot 9H_2O$ is simulated rather well using a parametric Hamiltonian. The crystal field splitting can be described in a good approximation by a D_{3h} symmetry. This high symmetry restricts the number of transitions found in the spectra. Although the concentration of Eu^{3+} ions is fairly high, the $^5D_2 \leftarrow {}^7F_1$ and $^5D_1 \leftarrow {}^7F_1$ transitions could not be observed. The weakness of the crystal field is mirrored in the small splittings of the multiplets. $Eu(BrO_3)_3 \cdot 9H_2O$ is one of the few examples where an overlap between the $^5L_6 \leftarrow {}^7F_0$ and $^5L_6 \leftarrow {}^7F_1$ transitions is absent. The weak crystal field reduces the importance of J-mixing. Crystal field transitions starting from the non-degenerate $^7F_0$ level and not obeying the Judd–Ofelt selection rule $|\Delta J| = 2, 4, 6$ [21] are sparse in the spectrum. So for instance the $^5D_3 \leftarrow {}^7F_0$ is not detected in $Eu(BrO_3)_3 \cdot 9H_2O$, whereas this transition can be seen in compounds with a strong crystal field, such as the rare earth garnets [22]. For the same reason, transitions to the $^5L_9$ and $^5L_{10}$ multiplets (27 800–28 500 cm^{-1}) are not observed.

The crystal field parameters of $Eu(BrO_3)_3 \cdot 9H_2O$ have been compared with those of other compounds in which the coordination polyhedron around the Eu^{3+} is an ideal or a distorted tricapped trigonal prism: $LaCl_3 : Eu^{3+}$ [23], $Eu(C_2H_5SO_4)_3 \cdot 9H_2O$ (EuES) [24], EuODA [13] and $Eu(OH)_3$ [25]. The parameters are given in table 5. Auzel's scalar crystal field strength parameters N_v [26] have been calculated too:

$$N_v = \left[\sum_{k,q} (B_q^k)^2 \left(\frac{4\pi}{2k+1} \right) \right]^{1/2}. \tag{4}$$

Table 4. Experimental and calculated crystal field levels for Eu^{3+} in $Eu(BrO_3)_3 \cdot 9H_2O$. The experimental ^7F_J levels are taken from Hasunuma *et al* [9]. The crystal field levels are calculated with the parameters from table 3 and labelled according to a D_{3h} symmetry.

$^{2S+1}L_J$	Symmetry label	E_{exp} (cm^{-1})	E_{calc} (cm^{-1})
$^7F_0$	Γ_1	0	−2
$^7F_1$	Γ_5	353	363
	Γ_2	405	413
$^7F_2$	Γ_6	1024	1026
	Γ_5	1038	1033
	Γ_1	1084	1084
$^7F_3$	Γ_4	1842	1828
	Γ_2	1882	1872
	Γ_6	1890	1881
	Γ_5	1918	1911
	Γ_3	1934	1922
$^7F_4$	Γ_6^a	2749	2739
	Γ_4	2812	2806
	Γ_5	2846	2839
	Γ_1	2911	2891
	Γ_6^b	2928	2919
	Γ_3	3075	3060
$^7F_5$	Γ_6^a	3844	3836
	Γ_2	3850	3830
	Γ_5^a	3860	3843
	Γ_4	3881	3874
	Γ_5^b	3979	3986
	Γ_6^b	4038	4021
	Γ_3	4079	4070
$^7F_6$	Γ_4	4928	4923
	Γ_6^a	4943	4941
	Γ_5^a	4979	4969
	Γ_1^a	4984	4980
	Γ_3	4991	4989
	Γ_6^b	5003	5003
	Γ_5^b	5050	5047
	Γ_1^b	5110	5099
	Γ_2	5112	5100
$^5D_0$	Γ_1	17 248	17 259
$^5D_1$	Γ_5	19 010	19 002
	Γ_2	19 019	19 013
$^5D_2$	Γ_1	—	21 469
	Γ_6	21 485	21 474
	Γ_5	—	21 479
$^5D_3$	Γ_3	—	24 342
	Γ_2	—	24 346
	Γ_6	24 342	24 347
	Γ_5	24 356	24 356
	Γ_4	—	24 377
$^5L_6$	Γ_1^a	—	25 064
	Γ_5^a	25 076	25 085
	Γ_6^a	25 129	25 127
	Γ_2	—	25 130
	Γ_3	25 145	25 149
	Γ_1^b	—	25 151
	Γ_5^b	25 171	25 179

Table 4. (Continued)

$^{2S+1}L_J$	Symmetry label	E_{exp} (cm^{-1})	E_{calc} (cm^{-1})
	Γ_6^b	25 263	25 248
	Γ_4	25 299	25 283
*			
$^5D_4$	Γ_3	27 555	27 569
	Γ_6^a	27 591	27 604
	Γ_4	27 592	27 605
	Γ_1	—	27 612
	Γ_5	—	27 613
	Γ_6^b	27 630	27 649
†			
$^3H_{3,4,5,6,7}$	Γ_3	30 923	30 920
	Γ_5	30 977	30 999
	Γ_4	31 000	31 010
	Γ_6	31 058	31 066
	Γ_4	31 095	31 093
	Γ_6	31 148	31 142
	Γ_6	31 448	31 463
	Γ_4	31 468	31 457
	Γ_4	31 526	31 520
	Γ_6	31 590	31 598
‡			

* 49 crystal field levels are calculated between 26 000 and 27 200 cm^{-1}; nine of them are found in the spectrum. These levels belong to the multiplets $^5L_7$, $^5G_2$, $^5G_3$, $^5G_4$, $^5G_5$, $^5G_6$ and $^5L_8$.
† Between 27 800 and 28 500 cm^{-1} the crystal field levels of the multiplets $^5L_9$ and $^5L_{10}$ are calculated. None is seen in the spectrum.
‡ In the range 32 800–35 100 cm^{-1}, the multiplets $^3P_0$, $^5F_1$, $^5F_2$, $^5F_3$, $^5I_4$, $^5I_5$ and $^5I_6$ are predicted. From the 55 calculated crystal field levels, we have detected 17 levels in the spectrum.

Table 5. B_q^k crystal field parameters (in cm^{-1}) for systems in which the coordination polyhedron around the Eu^{3+} is an ideal or distorted tricapped trigonal prism. The parameters are converted to our choice of the coordinate axis and to the C_q^k formalism. This explains the negative value for the B_6^6 parameter. Auzel's scalar crystal field strength parameter N_v (in cm^{-1}) [26] has been calculated also.

	$Eu(BrO_3)_3 \cdot 9H_2O$ (this work)	$Eu(BrO_3)_3 \cdot 9H_2O$ [9]	$LaCl_3 : Eu^{3+}$ [23]	EuES [24]	EuODA [13]	$Eu(OH)_3 : Eu^{3+}$ [25]
B_0^2	205	202	193	122	57	422
B_0^4	−279	−282	−296	−427	−895	−568
B_3^4	—	−3	—	—	−706	—
B_0^6	−557	−522	−818	−597	−415	−864
B_3^6	—	77	—	—	−664	—
B_6^6	−872	−859	−521	−600	−665	−649
N_v	1118	1079	1061	992	1686	1424

The crystal field parameters of $Eu(BrO_3)_3 \cdot 9H_2O$ are very comparable to those of EuES and especially to those of $LaCl_3 : Eu^{3+}$. The fact that the parameters for $Eu(BrO_3)_3 \cdot 9H_2O$ and EuES have the same sign and magnitude is not very surprising, since for both compounds the first coordination sphere around the europium ion contains nine water molecules. Although the direct environment of Eu^{3+} in $LaCl_3$ is from a chemical viewpoint totally different

Table 6. The scalar crystal field strength parameter N_v (in cm^{-1}) [26] for Eu^{3+} in different crystalline host matrices. The crystals are sorted according to increasing values for N_v.

Crystal	N_v (cm^{-1})	Reference
$Eu(C_2H_5SO_4)_3 \cdot 9H_2O$	992	[24]
$LaCl_3 : Eu^{3+}$	1061	[23]
$Eu(BrO_3)_3 \cdot 9H_2O$	1118	(this work)
$GdAsO_4 : Eu^{3+}$	1121	[28]
$YAsO_4 : Eu^{3+}$	1202	[28]
$LuPO_4 : Eu^{3+}$	1244	[28]
$YPO_4 : Eu^{3+}$	1266	[28]
$YVO_4 : Eu^{3+}$	1291	[28]
$Eu(OH)_3$	1424	[25]
$LaF_3 : Eu^{3+}$	1609	[17]
EuODA	1686	[13]
$YOOH : Eu^{3+}$	1768	[29]
$LiYF_4 : Eu^{3+}$	1798	[12]
$KY_3F_{10} : Eu^{3+}$	1927	[30]
$Y_2O_2S : Eu^{3+}$	1943	[31]
$GdBGeO_5 : Eu^{3+}$	2154	[32]
$YOCl : Eu^{3+}$	2175	[33]
$GdOCl : Eu^{3+}$	2187	[33]
$YOBr : Eu^{3+}$	2399	[34]
$LaONO_3 : Eu^{3+}$	2446	[35]
$GdONO_3 : Eu^{3+}$	2464	[35]
$GdOBr : Eu^{3+}$	2493	[34]
$LaOCl : Eu^{3+}$	2522	[33]
$LaOBr : Eu^{3+}$	2878	[34]
$Cs_2NaEuCl_6$	2901	[36]
LaOI	2914	[34]
$Y_3Al_5O_{12} : Eu^{3+}$	2967	[19]
Rb_2NaEuF_6	3722	[36]
Cs_2KYEuF_6	3912	[36]

from the environment of Eu^{3+} in $Eu(BrO_3)_3 \cdot 9H_2O$, the same weak crystal field splitting is found for both compounds. The N_v parameters of $Eu(BrO_3)_3 \cdot 9H_2O$, $LaCl_3 : Eu^{3+}$ and EuES are the smallest among the N_v parameters for the different europium systems (see table 6). Even the values for EuODA and $Eu(OH)_3$ are not very high. We can conclude that a tricapped trigonal prism as a coordination polyhedron (C.N. = 9) results in weak crystal fields, regardless of the chemical nature of the ligands. It is difficult to give a qualitative explanation for the small values of the crystal field parameters. The magnitude of the crystal field parameters depends on different factors, such as the charge of the ligands, the metal-to-ligand distances and the angles between different metal–ligand bonds. Recently, we have been able to give an explanation for the small values of second-rank crystal field parameters ($k = 2$), which describe the crystal field splitting of $J = 1$ manifolds ($^7F_1$ and $^5D_1$) [27]. Here, a small value of the B_0^2 crystal field parameter is due to special angular positions of the ligands.

Acknowledgments

KB is a research assistant of the Belgian National Fund for Scientific Research (NFWO). Financial support from the Geconcerteerde Onderzoeksakties (Konventie No 87 93-110) and from the IIKW (4.0007.94 and G.0124.95) is gratefully acknowledged.

References

[1] Bünzli J C G 1989 *Lanthanide Probes in Life, Chemical and Earth Sciences* ed J C G Bünzli and G R Choppin (Amsterdam: Elsevier) p 219
[2] Helmholtz L 1939 *J. Am. Chem. Soc.* **61** 1544
[3] Hellwege K H and Kahle H G 1951 *Z. Phys.* **129** 85
[4] Satten R A 1953 *J. Chem. Phys.* **21** 637
[5] Sikka S K 1969 *Acta Crystallogr.* A **25** 621
[6] Albertsson J and Elding I 1977 *Acta Crystallogr.* B **33** 1460
[7] Kato Y, Okada K, Fukuzaki H and Takenaka T 1978 *J. Mol. Struct.* **49** 57
[8] 1978 *Gmelin Handbuch der Anorganischen Chemie* vol C6, ed H Bergmann (Berlin: Springer)
[9] Hasunuma M, Okada K and Kato Y 1984 *Bull. Chem. Soc. Japan* **57** 3036
[10] Moret E, Nicolo F, Bünzli J C and Chapuis G 1991 *J. Less-Common Met.* **171** 273
[11] Görller-Walrand C, Hendrickx I, Fluyt L, Gos M P, D'Olieslager J and Blasse G 1992 *J. Chem. Phys.* **96** 5650
[12] Görller-Walrand C, Binnemans K and Fluyt L 1993 *J. Phys.: Condens. Matter* **5** 8359
[13] Görller-Walrand C, Verhoeven P, D'Olieslager J, Fluyt L and Binnemans K 1994 *J. Chem. Phys.* **100** 815; *J. Chem. Phys.* **101** 7189 (erratum)
[14] Görller-Walrand C, Vandevelde P, Hendrickx I, Porcher P, Krupa J C and King G S D 1988 *Inorg. Chim. Acta* **143** 259
[15] Görller-Walrand C, Huygen E, Binnemans K and Fluyt L 1994 *J. Phys.: Condens. Matter* **6** 7797
[16] Koster G F, Dimmock J O, Wheeler R G and Statz H 1963 *Properties of the Thirty-two Point Groups* (Cambridge, MA: MIT Press)
[17] Carnall W T, Goodman G L, Rajnak K and Rana R S 1989 *J. Chem. Phys.* **90** 3443
[18] Wybourne B G 1965 *Spectroscopic Properties of Rare Earths* (New York: Wiley)
[19] Görller-Walrand C and Binnemans K Rationalization of crystal field parametrization *Handbook on the Physics and Chemistry of Rare Earths* ed K Gschneidner Jr and L Eyring (Amsterdam: North-Holland) at press
[20] Judd B R and Crosswhite H 1984 *J. Opt. Soc. Am.* B **1** 255
[21] Peacock R D 1975 *Struct. Bonding* **22** 83
[22] Binnemans K and Görller-Walrand C 1995 unpublished results
[23] DeShazer L G and Dieke G H 1963 *J. Chem. Phys.* **38** 2190
[24] Hammond R M, Reid M F and Richardson F S 1989 *J. Less-Common Met.* **148** 311
[25] Cone R L and Faulhaber R 1971 *J. Chem. Phys.* **55** 5198
[26] Auzel F and Malta O L 1983 *J. Physique* **44** 201
[27] Binnemans K and Görller-Walrand C 1995 *Chem. Phys. Lett.* **245** 75
[28] Linarès C, Louat A and Blanchard M 1977 *Struct. Bonding* **33** 179
[29] Hölsä J 1990 *Z. Naturf.* a **45** 173
[30] Porcher P and Caro P 1976 *J. Chem. Phys.* **65** 89
[31] Sovers O J and Yoshioka T 1969 *J. Chem. Phys.* **51** 5330
[32] Antic-Fidancev E, Serhan K, Taibi M, Lemaitre-Blaise M, Porcher P, Aride J and Boukhari A 1994 *J. Phys.: Condens. Matter* **6** 6852
[33] Hölsä J and Porcher P 1981 *J. Chem. Phys.* **74** 2108
[34] Hölsä J and Porcher P 1982 *J. Chem. Phys.* **76** 2790
[35] Hölsä J, Karppinen M and Kestilä E 1994 *J. Alloys Compounds* **207/208** 64
[36] Tanner P A, Ravi Kanth Kumar V V, Jayasankar C K and Reid M F 1994 *J. Alloys Compounds* **215** 349